Phylogenetic revision of the shrimp genera *Ephyrina, Meningodora* and *Notostomus* (Acanthephyridae: Caridea)

ANASTASIIA A. LUNINA◻, DMITRY N. KULAGIN and ALEXANDER L. VERESHCHAKA*

Shirshov Institute of Oceanology, Russian Academy of Sciences, Nakhimovski Prospekt 36, Moscow, 117997, Russia

The shrimp genera *Ephyrina*, *Meningodora* and *Notostomus* have an unusual carapace strengthened with carinae and a half-serrated mandible, which may suggest a possible monophyly of this group. Here we test this hypothesis and present the first phylogenetic study of these genera based on 95 morphological characters (all valid species coded) and six molecular markers (71% of valid species sequenced). Representatives of all genera of Oplophoridae (sister to Acanthephyridae) were outgroups, 32 species belonging to all genera and potentially different clades of Acanthephyridae were ingroups. Both morphological and molecular analyses retrieve trees with similar topology. Our results reject the hypothesis of a clade formed by *Ephyrina* + *Meningodora* + *Notostomus*. We show that *Ephyrina* and *Notostomus* are monophyletic, both on morphological and on molecular trees, *Meningodora* gains support only on morphological trees. Evolutionary traits in the *Ephyrina* and *Meningodora* + *Notostomus* clades are different. Synapomorphies are mostly linked to adaptations to forward motion in *Ephyrina* (oar-like meri and ischia of pereopods, stempost-like rostrum) and to progressive strengthening of the carapace and pleon in *Meningodora* and *Notostomus* (net of sharp carinae). Unusual mandibles evolved in the clades independently and represent convergent adaptations to feeding on gelatinous organisms.

ADDITIONAL KEYWORDS: Crustacea – evolution – phylogeny – plankton biology – shrimp.

INTRODUCTION

Among pelagic decapods, Oplophoroidea is one of the most diverse superfamilies occurring in the widest geographic and depth ranges. Indeed, nearly one hundred species have been recorded from polar to equatorial regions (WoRMS, 2020), from the upper mixed layer to bathyal depths. Their role in pelagic trophic chains is important: Oplophoroidea are a dominant group explaining nearly half of the total zooplankton stock in the Atlantic tropical and equatorial waters (Vereshchaka *et al.*, 2019b).

Historically, Oplophoroidea was considered on morphological grounds as a single family Oplophoridae (e.g. Chace, 1986; De Grave *et al.*, 2009), but molecular data suggest that it consists of two families, Oplophoridae and Acanthephyridae, within the superfamily Oplophoroidea (e.g. Bracken *et al.*, 2009; Chan *et al.*, 2010; Lunina *et al.*, 2019b; WoRMS, 2020).

Following this two-family concept, we have revised the global fauna of the family Oplophoridae (Lunina *et al.*, 2019b) and now take the next step to start a phylogenetic revision of the family Acanthephyridae, which is more species-rich than Oplophoridae (55 vs. 16 currently accepted species, seven vs. three genera; WoRMS, 2020).

Acanthephyridae is morphologically heterogeneous in many aspects (Chace, 1986). For example, the rostrum may have more teeth on the ventral than on the dorsal margin (*Heterogenys* Chace, 1986) or vice versa (other genera), the hepatic spine and three lateral carinae on the carapace may be present (*Kemphyra* Chace, 1986) or absent (other genera), the carapace is ventrally dentate (*Notostomus* A. Milne-Edwards, 1881) or smooth (other genera), the dorsal pleonic carina is absent (*Ephyrina* Smith, 1885 and *Hymenodora* Sars, 1877) or developed (other genera), eggs are large and few (< 50) (*Ephyrina* and *Hymenodora*) or small and numerous (> 80) (other genera). One of the basic phylogenetic characters in Crustacea, the morphology of the mandible, also varies. In Acanthephyridae, this

*Corresponding author. E-mail: alv@ocean.ru

character, which is conservative in decapods at family and even superfamily level, may have two different states (Chace, 1986): (1) subtriangular and armed along the entire margin (Fig. 1A) and (2) subtruncate and unarmed in the distal half beyond the apex, except the terminal tooth (Fig. 1B). The first state is common for most pelagic carnivorous shrimps (Burukovsky, 2009), while the second state is restricted only to the genera *Ephyrina*, *Meningodora* Smith, 1882 and *Notostomus*; its adaptive value has never been assessed. In addition to the remarkable mandible, *Ephyrina*, *Meningodora*

and *Notostomus* are characterized by strong ridges and carinae along the lateral sides of the carapace (Fig. 1C–E). These structures are also unusual for most pelagic shrimps, having a more or less smooth and streamlined carapace. Both unusual characters (a half-serrated mandible and a strengthened carapace) may suggest possible monophyly of this group. Here we test this hypothesis and thus start a revision of the global Acanthephyridae fauna. Using morphological and molecular data, we examine whether the unusual mandible and the strengthened carapace represent
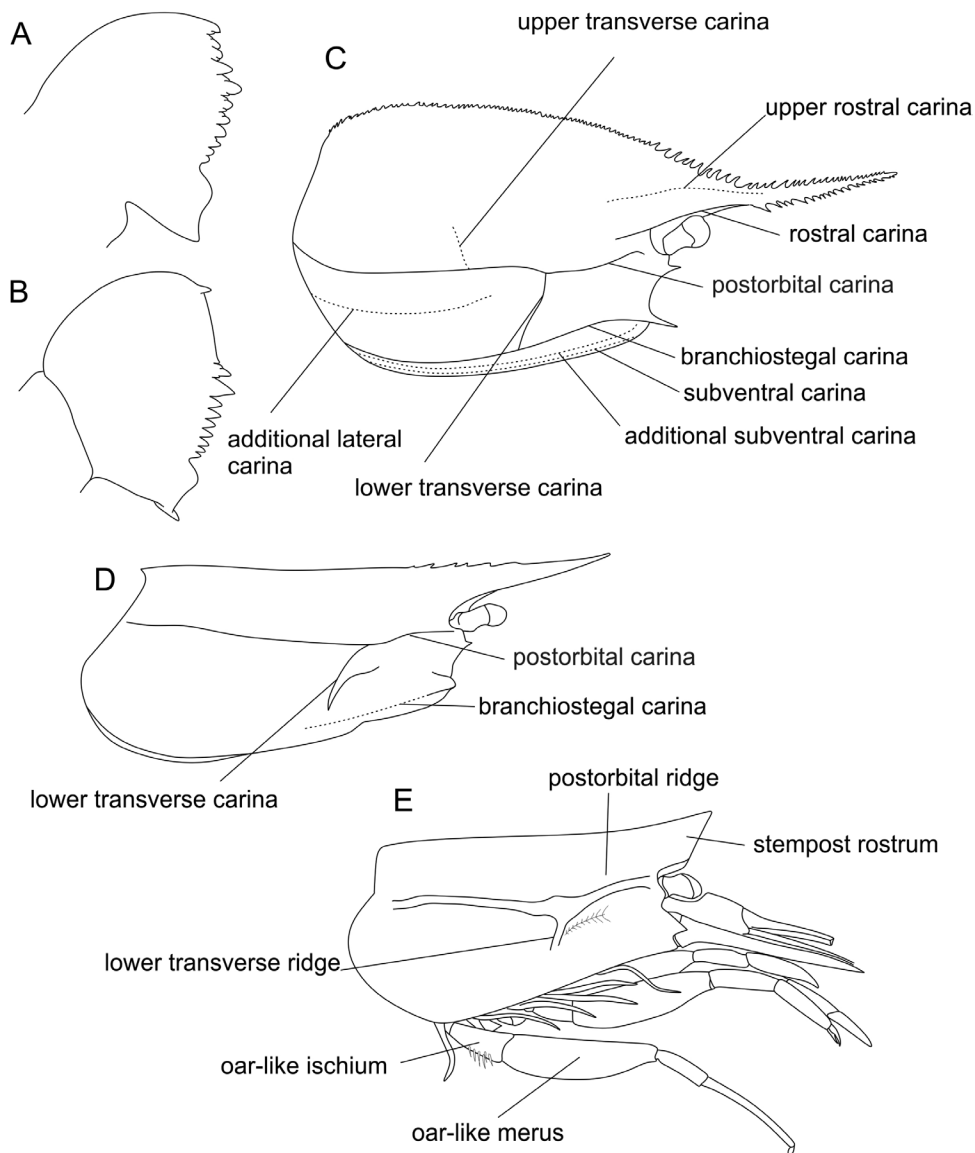
Figure 1. Morphological characters of Acanthephyridae. A, typical mandible of Oplophoroidea (exemplified by *Acanthephyra brevicarinata*). B, mandible of the *Ephyrina–Meningodora–Notostomus* group (exemplified by *Ephyrina bifida*). C, schematic carapace view of *Notostomus* (exemplified by *N. elegans*). D, schematic carapace view of *Meningodora* (exemplified by *M. compsa*). E, schematic carapace view of *Ephyrina* (exemplified by *E. bifida*). Dotted lines indicate additional carinae, which are present alongside the obligatorily carinae (solid lines) in part of species.

synapomorphies of a single clade or if they evolved independently in separate clades.

Among 21 currently accepted species of the *Ephyrina–Meningodora–Notostomus* group (WoRMS, 2020), none has been included in previous morphological phylogenetic analyses and only a few were included in molecular analyses: a single one (Bracken *et al.*, 2009), two (Chan *et al.*, 2010) or seven species (Wong *et al.*, 2015). The previous molecular analyses targeted higher level relationships within Caridea and/or Oplophoroidea, and did not cover the proper diversity of the *Ephyrina–Meningodora–Notostomus* group. Here we present the first comprehensive phylogenetic analysis based on the simultaneous use of morphological characters and molecular markers. We used 95 morphological characters to encode all valid species of the target genera, and six gene markers for 15 species (71% of currently accepted species). We also included in the analyses representatives of all three genera of Oplophoridae (outgroups). *Acanthephyra* A. Milne-Edwards, 1881, which is morphologically variable and probably polyphyletic (Chace, 1986), was represented in our analysis by 12 species from morphologically different groups.

MATERIAL AND METHODS

MORPHOLOGICAL ANALYSIS

Oplophoridae encompasses three genera (*Janicella* Chace, 1986, *Oplophorus* Milne-Edwards, 1837 and *Systellaspis* Spence Bate, 1888) and is considered as a sister-clade to Acanthephyridae (Wong *et al.*, 2015), which includes, in addition to the three analysed genera, *Acanthephyra*, *Heterogenys*, *Hymenodora* and *Kemphyra*. We chose as the outgroups representatives of the three genera of Oplophoridae: *Janicella spinicauda* (A. Milne-Edwards, 1883) (Analysis 1), *Oplophorus gracilirostris* A. Milne-Edwards, 1881 (Analysis 2) and *Systellaspis pellucida* (Filhol, 1884) (Analysis 3).

We included as the ingroups all valid species of *Ephyrina* (six species), *Meningodora* (six) and *Notostomus* (nine), and representatives of all other genera of Acanthephyridae; the highly diverse and probably polyphyletic (Chace, 1986) genus *Acanthephyra* was represented by 12 species from potentially different clades (Table 1).

For each included taxon we identified and encoded 95 morphological characters (not weighted, Supporting Information, Appendix S1), which were combined into four morphological groups (Fig. 2): carapace (characters 0–32 in Supporting Information, Appendix S1), pleon + telson (33–55), mouthparts (58–74) and pereopods (75–92).

The dataset (Supporting Information, Appendix S2) was handled and analysed using a combination of programs using maximum parsimony settings: WINCLADA/NONA and TNT (Nixon, 1999; Goloboff *et al.*, 2000). Trees were generated in TNT with 30 000 trees in memory, under the 'traditional search' (branch-and-bound) algorithms. Relative stability of clades was assessed by standard bootstrapping (sample with replacement) with 10 000 pseudoreplicates and by Bremer support (algorithm TBR, saving up to 10 000 trees up to 12 steps longer). In all analyses, clades were considered robust if they had synchronously Bremer support ≥ 3 and bootstrap support ≥ 70.

MOLECULAR ANALYSIS

We used both original data (15 species across six genera) and sequences from GenBank (22 species across six genera) (Table 2). All seven genera of the family are thus represented in the molecular dataset. Outgroups and ingroups were the same as in the morphological analysis (Table 2).

We selected six molecular markers: a mitochondrial ribosomal gene (16S), a mitochondrial protein-coding gene (cytochrome *c* oxidase subunit I, *COI*), a nuclear ribosomal gene (18S) and three nuclear protein-coding genes: histone *H3*, sodium-potassium ATPase alpha-subunit (NaK, ~565 bps) and phosphoenolpyruvate carboxykinase (PEPCK). These markers have been widely applied in decapod phylogenetic analyses and proven to be informative at fine and coarse evolutionary scales (Bracken *et al.*, 2009; Felder & Robles, 2009; Robles *et al.*, 2009; Toon *et al.*, 2009; Bracken-Grissom *et al.*, 2014; Ditter *et al.*, 2020).

Total genomic DNA was extracted from the pleopods or abdomen using the Qiagen DNeasy Blood and Tissue Kit in accordance with the manufacturer's protocol. Polymerase chain reaction (PCR) amplification of the *COI* gene was performed with the primers: COL6/COH6 (~ 650 bps; Schubart & Huber, 2006; Schubart, 2009) or L*COI* 1490/H*COI* 2198 (~ 650 bps, Folmer *et al.*, 1994). The mitochondrial large subunit 16S rRNA was amplified by 16L2/16*H*3 primers (~550 bps; Schubart *et al.*, 2002; Reuschel & Schubart, 2006), and the nuclear small subunit 18S rRNA was amplified by A/L, C/Y, O/B primers (~1800 bps; Apakupakul *et al.*, 1999). Nuclear *H3* gene fragment was amplified by *H3*A/*H3*B primers (~330 bps; Colgan *et al.*, 1998), NaK with primers for-b/rev2 (~660 bps; Tsang *et al.*, 2008) and PEPCK (~510 bps) with the 5' primer PEPCK for (Tsang *et al.*, 2008) and newly designed for this study PEPCK acant-rev2 (5'-RCCR AAGTTGTARCCAAAGAAGGG-3') as the 3' primer. Polymerase chain reaction amplification reactions were performed in 25 µL containing 1 × PCR buffer, 1 µL of 10 µmol/L of primer pair mix, 1 µL of DNA

Table 1. Individuals used in morphological analyses. MNHN, National Museum of Natural History (Paris, France); NMNH, National Museum of Natural History, Washington, D.C., United States; ZMUK, National History Museum, Copenhagen, Denmark; IO RAN, Institute of Oceanology, Russian Academy of Scienses

Species	Coordinates	Other information	Museum, number
Acanthephyra acutifrons	14° 43'N; 45° 02' W	'Professor Logatchev' 39 cruise St 215 RT, RTAK	IO RAN 39L 215 RT №1
Acanthephyra acutifrons	8°53'S, 159°23'E	Océanie, Salomon, New Georgia sound, SALOMONBOA 3, N.O. 'Alis', CP2783, prof. 1501–1545 m. 13.09.2007	MNHN-IU-2016-9247
Acanthephyra armata	06°56'N, 52°35'W	N.O. 'Hermano Gines' GUYANE 2014 Stn CP4405 555–597 m, MNHN-convention APA-973-1, 09.08.2014	MNHN-IU-2013-2686
Acanthephyra armata	06°36'N, 52°35'W	N.O. 'Hermano Gines' GUYANE 2014 Stn CP4405 555–597 m, MNHN-convention APA-973-1, 09.08.2014	MNHN-IU-2016-9261
Acanthephyra armata	06°36'N, 52°35'W	N.O. 'Hermano Gines' GUYANE 2014 Stn CP4405 555–597 m, MNHN-convention APA-973-1, 09.08.2014	MNHN-IU-2016-9261
Acanthephyra carinata	05°27'S, 145°56'E	Papouasie Nouvelle-Guinée: Astrolabe Bay, N.O. 'Alis', BIOPAPUA. Stn CP3717, 850–945 m. 06.10.2010	MNHN-IU-2016-9274
Acanthephyra cucculata	16° 04 N'; 46° 41' W	39 cruise RV 'Logatchev', 14–15.03.2018, 1500–0 m	IO RAN 39L233RT №65
Acanthephyra curtirostris	35°37'96'E, 21°36'54'S	Afrique, Mozambique, Canal du Mozambique, Indien, Mainbasa, 'Vizconde de Eza', CP3147. Chalut a perche, prof. 990–996 m, 12.04.2009	MNHN-IU-2016-9280 (MNHN-Na-17146)
Acanthephyra curtirostris	14° 43' N; 45° 02' W	39 cruise RV 'Logatchev'	IO RAN39L215RT, №1
Acanthephyra fimbriata	12°09'N, 122°14'E	MUSORSTOM 3, Philippines. St. CP 136, 1404 m	MNHN-IU-2018-1565
Acanthephyra indica	8°11'N, 79°03'E	N.O. 'Marion Dufense' SAFARI II, St.04 CP06, 1035 m	MNHN-IU-2018-1566
Acanthephyra indica	12°57'S, 48°03'E	Campagne MIRIKY Madagascar, 'Miriky', entre Nosy-be et Banc du Leven, Stn CP3219, 01.07.09, 906–918 m.	MNHN-IU-2009-1905
Acanthephyra indica	21°36'54'S, 35°57'96'E	Afrique, Mozambique, Canal du Mozambique, Indien. Mainbaza, N.O. 'Vizconde de Eza', Campagne Mainbaza. Stn. CP3147, 990–996 m. 12.04.2009.	MNHN-IU-2008-10188
Acanthephyra media	13°05'N, 122°25'E	MUSORSTOM 2, Philippines. St. CP 42, 1580–1610 m	MNHN-IU-2018-1567
Acanthephyra pelagica	36°45'N, 0°16'E	DANA 1920–1922. St. 1128(1). S 200. 01.10.1921, 21.50.	ZMUK
Acanthephyra quadrispinosa	29°39'S, 44°16'E	Expedition ATIMO VATAE. SUD MADAGASCAR, Sud Pointe Barrow. Chaultier 'Nosy Be 11', Stn. CP 3596, 986–911 m. 12.05.2010.	MNHN-IU-2010-4285
Acanthephyra quadrispinosa	29°39'S, 44°16'E	Expedition ATIMO VATAE. SUD MADAGASCAR, Sud Pointe Barrow. Chaultier 'Nosy Be 11', Stn. CP 3596, 986–911 m. 12.05.2010.	MNHN-IU-2010-4285
Ephyrina benedicti	2°39'S, 5°43'2E	Campagne WALDA Prélèvement 142Engin CY20, Chalut Blake Prof. 4088m. 27.07.1971.	MNHN-IU-2018-1582
Ephyrina bifida	28°41'N, 60°57'W	Anton Dohrn 92, St. 5780, 2000 m	ZMUK
Ephyrina bifida	39°39,1'N, 15°00,2'W	ABYPLANE St CP15, chalutage 5320 m, 9.06.1981, 8h07–9H30	MNHN-IU-2018-1580
Ephyrina figueirai	05°27'S, 146°09'E	Bismarck Sea: Basamuk Bay, N.O.'Alis', Expedition PAPUA NIUGINI, Stn CP4082, 800–1065 m, 26/12/2012	MNHN-IU-2013-8725
Ephyrina ombango	10°23,17'N, 46°45,34'W	DEMERABY, CP07, chalutage 4850 m. 20.09.80	MNHN-IU-2018-1579
Ephyrina ombango	9°18'S, 11°10'E	'Ombango', C14, St.325,midwater traul, 0–725 m, 02.03.1961, 23h00–23h15	MNHN-IU-2014-11098
Hymenodora glacialis	02°03'S, 118°45'E	Indonésie, CORINDON -Makassar. St CH286, 1710–1730 m	Na 10655

Table 1. Continued

| Species	Coordinates	Other information	Museum, number
Hymenodora glacialis	73°28'N, 10°07'W	Mer de Norvège, Campagne NORBI, N.O. 'Jean Charcot', Stn CP16, 2937 m, 07.08.1975	MNHN-IU-2008–16833
Hymenodora gracilis	37°39'S, 77°26'E	Ile Amsterdam, Campagne Jasus (MD 50), N.O. 'Marion Dufresne', Stn CP193, 2800–3075 m. 27.06.1986	MNHN-IU-2008–16839
Janicella spinicauda	1°28'S, 48°06'E	ROV 'Vityaz', 17th cruise, St. 2604,13.11.88, 670–690 m	ZMUK
Janicella spinicauda	8°44'S, 43°54'E	Dana Expedition, St. 3939-1, 23.12.1929, 500 meter wire	ZMUK
Kemphyra corallina	37°54'S, 77°22'E	Iles St Paul et Amsterdam, 'Marion Dufresne' Cne MD Jasus Stn CP 56. 2280–2310 m. 14.07.1986. 20h02–22*H*31	MNHN-IU-2018-1581
Kemphyra corallina	33°59'S, 43°55'E	Indian Ocean: Walters shoal, Plaine Sud. N.O. 'Marion Dufresne', Campagne MD208(Walters Shoal). Stn CP49156, 1865–2058 m, 12.05.2017	MNHN-IU-2016–9402
Meningodora compsa	16°16'N, 22°16'W	Service de l'élevage du Sénégal. M.W.T. 0–1000 m. 16.01.1959	MNHN-IU-2018-1577
Meningodora longiscula	9°55'N, 142°00'E	Nouvelle-Calédonie, Campagne Caride V. Stn 15, 1000 m., 12.09.1969	MNHN-IU-2011–5635
Meningodora mollis	34°06'N, 17°06'W	North Atlantic, Campagne Abyplane, N.O. 'Cryos',Stn. CP11, 4270 m, 30.05.1981	MNHN-IU-2011–5640
Meningodora vesca	39°59'N, 15°00'W	North Atlantic, Campagne ABYPLANE, N.O. 'Cryos', STN CP15, 5320 m	MNHN-IU-2011–5634
Notostomus auriculatus	33°59'S, 43°55'E	Indian Ocean: Walters shoal, Plaine Sud. N.O. 'Marion Dufresne', Campagne MD208(Walters Shoal). Stn CP4915, 1865–2058 m, 12.05.2017	MNHN-IU-2016–9404
Notostomus elegans	21°46'S, 36°35'E	37 cruise RV Logatchev, St 156 TS	IO RAN
Notostomus gibbosus	54°11'19N, 166°45'37'W	Afrique, Mozambique, Canal du Mozambique, Indien, Campagne Mainbasa, N.O. 'Vizconde de Eza', Stn CC3156, 1810–1820, 14.04.2009	MNHN-IU-2008–10189
Notostomus japonicus	29°50,9S, 48°35,5E	North Pacific Ocean, Bering Sea, Alaska. 19.05.2001. NOAA Expedition 2001, R/V Vesteraalen. Depth 628 m.	USNM 1164652
Notostomus murrayi	31°12,0S, 39°18,0W	SUD/SUD-EST MADAGASCAR, Campagne Safari I(MD20), N.O. 'Marion Dufresne, St.18, CP10, 04.09.1979, 7:36–8:20, 3668–3800 m	MNHN-IU-2011–5686
Notostomus murrayi	37°08'24'N, 074°17'42'W	ASV46, St 2719, 800–200 m, 25.10.2018	IO RAN 9-D2
Notostomus robustus	25°11'N, 122°35'E	North Atlantic ocean, United States, North American slope, Off Virginia. Trawl. Depth 2933 ms. Gilliss R/V GI-75-08-35. 14.09.1973	USNM 222196
Oplophorus gracilirostris	20°08'N, 82°59'W	Dana Expedition, St. 3722–3, 300 meter wire	ZMUK
Oplophorus gracilirostris	12°30'S, 48°16'E	Dana Expedition, St. 1218, 800 meter wire	ZMUK
Oplophorus gracilirostris	22°06'N, 84°58'W	ROV 'Vityaz', 17th cruise, St. 2597, 12.11.88, 360–555 meter wire.	ZMUK
Oplophorus gracilirostris	35°47'N, 05°17'W	Dana Expedition, St. 1223, 500 metre wire	ZMUK
Pasiphaea sivado	No data	Detroit de Gibraltar, N.O. 'Cryos', BALGIM, St. CP150, 280–300 m, 18.06.1984	MNHN-IU-2018-1611
Penaeus monodon	7°55'S, 12°38'E	Andrea 1877, Singapore	ZMUK
Solenocera membranaceum	2°15'S, 98°55,5'E	Atlantide Exp. West Africa 1945–1946. St. 135, depth 460–235 m, Gear: ET, 17.03.1946, 13:40–15:40.	ZMUK
Systellaspis debilis		Dana Expedition, St. 3817-3, 11.09.1929, 300 metre wire	ZMUK

Table 1. Continued

Species	Coordinates	Other information	Museum, number
Systellaspis debilis	17°10'N, 46°25'W	ROV 'Professor Logachev', 37 cruise, St. 99 IKMT	IO RAN 37L99 IKMT
Systellaspis debilis	21°57'N; 22°58'W	Dana Expedition, St. 1157, E 300, 27.10.1921	ZMUK
Systellaspis debilis	31°12.0S, 39°18.0W	R.V. Akademik Sergey Vavilov, 46 cruise, St. 2719, 25.10.2018, 200–800 m	IO RAN 13-D1

template, 0.2 mmol/L of each dNTP and 0.5 units of Taq polymerase. The thermal profile used an initial denaturation for 3 min at 95 °C followed by 35–40 cycles of 20 s at 94 °C, 30 s at 45–57 °C depending on primer pair, 1 min at 72 °C and a final extension of 7 min at 72 °C. Polymerase chain reaction products were purified using the PCR Purification Kit protocol (Promega) and sequenced in both directions using BigDye Terminator v.3.1 (Applied Biosystems). Each sequencing reaction mixture, including 0.5 µL of BigDye Terminator v.3.1, 0.8 µL of 1 µmol/L primer and 1–2 µL of purified PCR template, was run for 30 cycles of 96 °C (10 s), 50 °C (5 s) and 60 °C (4 min). Sequences were purified by ethanol precipitation to remove unincorporated primers and dyes. Products were re-suspended in 14 µL formamide and electrophoresed in ABI Prism-3500 sequencer (Applied Biosystems). The nucleotide sequences were cleaned and assembled using CodonCode Aligner v.7.1.1. Protein-coding sequences (*COI*, *H3*, NaK and PEPCK) were checked for indels and stop codons to prevent the inclusion of pseudogenes. All sequences were then compared to genes reported in GenBank using BLAST (National Center for Biotechnology Information, NCBI) to check for potential contamination.

For each gene-fragment, the sequences were aligned using MUSCLE (Edgar, 2004) implemented in MEGA v.X (Kumar *et al.*, 2018), and the alignment accuracy was adjusted by eye. Missing data were designated with a '?' for any incomplete sequences. All obtained sequences were submitted to the NCBI GenBank database (Table 2).

To assess phylogenetic relationships between species, Bayesian inference (BI) and maximum likelihood (ML) analyses were run. The BI analysis was conducted in MrBayes v.3.2.6 (Ronquist *et al.*, 2012) for the concatenated dataset of all genes. The combined dataset was partitioned and analysed using models selected by PartitionFinder2 (Lanfear *et al.*, 2016). Akaike information criterion (AICc modification for small sample size) metric implemented in PartitionFinder2 was used to obtain the optimal partitioning scheme. Two independent runs, each consisting of four chains, were executed for this analysis. A total of 10 000 000 generations were performed for the combined dataset, with sampling every 1000 generations, and the first 25% trees (i.e. 2500 trees for combined dataset) were discarded as 'burn-in'. A 1% average standard deviation of split frequencies was reached after about 1.1 million generations.

The maximum likelihood (ML) analysis was run in RAxML GUI v.2.0 (Stamatakis, 2014; Edler *et al.*, 2020), and the GTR+G model was used. Bootstrap resampling with 1000 replicates was run using the thorough bootstrap procedure to assign support to
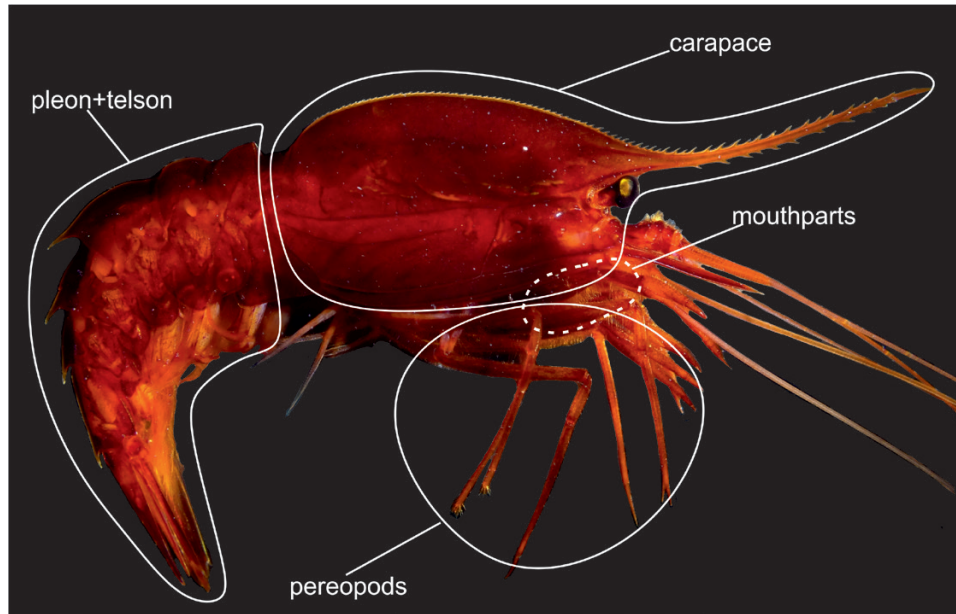
Figure 2. Grouping of morphological characters (schematic white lines) in *Ephyrina, Meningodora* and *Notostomus* exemplified by *Notostomus elegans*.

branches in the ML tree. Final ML tree was generated using the partitioned dataset of all concatenated genes.

We considered the clades statistically supported if they had a synchronous support of posterior probabilities ≥ 0.9 in the BI analysis and bootstrap value ≥ 70% in the ML analysis.

RESULTS

MORPHOLOGICAL ANALYSES

Analysis 1 with *Janicella spinicauda* as outgroup retrieved a single most-parsimonious (MP) tree (Fig. 3A; Supporting Information, Appendix S3) with a score of 109 (Ci = 88, Ri = 96). The tree shows that *Hymenodora* is a sister-clade to the rest of the genera, the latter clade includes two sister-clades: *Ephyrina* and *Heterogenys + Kemphyra + Acanthephyra + Notostomus + Meningodora*. There is also a well-supported clade *Meningodora + Notostomus* within which both genera are robust sister-clades. *Acanthephyra* shows polytomy.

Analysis 2 with *Oplophorus gracilirostris* as outgroup retrieved a single MP tree (Fig. 3B; Supporting Information, Appendix S3) with a score of 116 (Ci = 82, Ri = 95). Analysis 3 with *Systellaspis pellucida* as outgroup also retrieved a single MP tree (Fig. 3C; Supporting Information, Appendix S3) with a score of 104 (Ci = 92, Ri = 98). Both trees are similar in topology to each other and to the tree retrieved in Analysis 1, with the same set of statistically supported clades.

MOLECULAR ANALYSES

We successfully obtained 84 sequences across six gene fragments for 15 out of 21 species from the genera *Ephyrina*, *Meningodora* and *Notostomus*. In order to retrieve phylogenetic reconstructions, we also included all species of Acanthephyridae from GenBank with at least two selected gene markers. Prior to analyses, all sequences from GenBank were checked for contamination or possible misidentification using BLAST search and preliminary phylogenetic reconstruction with each gene separately. A total of 35 species from seven genera of Acanthephyridae and three genera of Oplophoridae were thus put in the data matrix. The concatenated six-marker dataset comprised 4525 bp. Results from PartitionFinder2 recommended a 12-partition scheme by gene and codon (*H3*, *COI*, NaK, PEPCK), which was used in the final analyses. Substitution models for each partition are listed in Table 3.

Molecular analysis retrieved Bayesian and ML trees, which are similar to each other in topology but significantly differ in support of two major clades (Fig. 4).

On the BI tree, *Hymenodora* is a sister-clade to the rest of the genera, the latter clade includes two sister-clades: *Ephyrina* and '*Heterogenys + Kemphyra + Acanthephyra + Notostomus + Meningodora*'. There is also a well-supported clade *Meningodora + Notostomus*, within which *Notostomus* is monophyletic and *Meningodora* shows polytomy. Although the BI tree shows polytomy of *Acanthephyra*, some clades

Table 2. Individuals used in phylogenetic reconstruction with localities, voucher numbers, and GenBank accession numbers. New sequences obtained are in bold, 'N' – sequences not acquired

Species	Voucher No	Locality/year	GenBank accession numbers						References
			COI	16S	18S	H3	NaK	PEPCK	
Ephyrina									
Ephyrina benedicti	ACP1	Central Atlantic / 2018	**MW043002**	**MW043446**	**MW043461**	N	**MW052302**	**MW052315**	This study
Ephyrina benedicti	HBG6799	Gulf of Mexico / 2016	MH572612	MH542965	N	N	N	N	Published in GenBank, Wilkins & Bracken-Grissom, 2020
Ephyrina bifida	HBG160	North Atlantic	KP076186	N	KP075779	N	KP076039	N	Wong *et al.*, 2015
Ephyrina figueirai	MNHN-IU-2013–8725 / ACP4	Papua New Guinea / 2012	**MW043003**	**MW043447**	**MW043462**	**MW052288**	**MW052303**	**MW052316**	This study
E. figueirai spinicauda	HBG933	Taiwan	KP076189	KP075911	KP075800	KP076105	KP076038	N	Wong *et al.*, 2015
Ephyrina ombango	ACP6	Central Atlantic / 2018	**MW043004**	**MW043448**	**MW043463**	**MW052289**	**MW052304**	**MW052317**	This study
Ephyrina ombango	HBG1230	Gulf of Mexico	KP076188	KP075914	KP075802	KP076107	N	N	Wong *et al.*, 2015
Heterogenys									
Heterogenys microphthalma	HBG937	Taiwan	KP076183	KP075898	KP075787	KP076124	KP076035	N	Wong *et al.*, 2015
Hymenodora									
Hymenodora glacialis		Arctic Ocean / 1975N		GQ131896	GQ131915	N	N	N	Chan *et al.*, 2010
Hymenodora gracilis	ACP12	Central Atlantic / 2018	**MW043005**	**MW043449**	**MW043464**	**MW052290**	**MW052305**	**MW052318**	This study
Kemphyra									
Kemphyra corallina	MNHN-IU-2016–9402/ACP46	South-West Indian Ocean / 2017	**MW043006**	**MW043450**	**MW043465**	**MW052291**	N	N	This study
Meningodora									
Meningodora compsa	HBG1241 and HBG7260	Gulf of Mexico	Unpublished, H. Bracken-Grissom	KP075907	KP075791	KP076114	N	N	Wong *et al.*, 2015
Meningodora longisulca	ACP19	Central Atlantic / 2016	**MW043007**	**MW043451**	**MW043466**	**MW052292**	**MW052306**	**MW052319**	This study
Meningodora miccyla	ACP17	Central Atlantic / 2018	**MW043008**	**MW043452**	**MW043467**	**MW052293**	**MW052307**	**MW052320**	This study
Meningodora mollis	HBG901	Gulf of Mexico	KP076192	KP075910	KP075783	KP076115	KP076033	N	Wong *et al.*, 2015
Meningodora mollis	HBG1170	Spain	KP076193	N	KP075813	KP076116	KP076034	N	Wong *et al.*, 2015
Meningodora vesca	ACP32	Central Atlantic / 2018	**MW043009**	**MW043453**	**MW043468**	**MW052294**	**MW052308**	**MW052321**	This study

Table 2. Continued

Species	Voucher No	Locality/year	GenBank accession numbers						References
			COI	16S	18S	H3	NaK	PEPCK	
Meningodora vesca	HBG4178	Gulf of Mexico	MF197254	MF197197	N	N	N	N	Published in GenBank, Wilkins & Bracken-Grissom, 2017
Notostomus									
Notostomus auriculatus	MNHN-IU-2016–9404/ACP20	South-West Indian Ocean / 2017	MW043010	MW043454	MW043469	MW052295	MW052309	MW052322	This study
Notostomus elegans	ACP23	Central Atlantic / 2016	MW043011	MW043455	MW043470	MW052296	MW052310	MW052323	This study
Notostomus elegans	HBG1232 and HBG1169	Gulf of Mexico	KP076194	KP075900	KP075803	KP076119	KP076034	N	Wong *et al*., 2015
Notostomus gibbosus	ACP35	Central Atlantic / 2015	MW043012	MW043456	MW043471	MW052297	MW052311	MW052324	This study
Notostomus gibbosus	HBG903A and HBG4220	Gulf of Mexico	MH572685	KP075905	KP075795	KP076120	N	N	Wong *et al*., 2015; Published in GenBank, Wilkins & Bracken-Grissom, 2020
Notostomus japonicus	USNM 1164652/ACP25	Bering Sea / 2001	DQ882094	MW043457	MW043472	MW052298	N	N	This study; Published in GenBank, Costa *et al*., 2018
Notostomus murrayi	ACP30	South Atlantic / 2018	MW043013	MW043458	MW043473	MW052299	MW052312	MW052325	This study
Notostomus robustus	ACP24	Central Atlantic / 2016	MW043014	MW043459	MW043474	MW052300	MW052313	MW052326	This study
Acanthephyra									
Acanthephyra acutifrons	HBG1254	Gulf of Mexico	KP076167	KP075874	KP075817	KP076084	KP076037	N	Wong *et al*., 2015
Acanthephyra armata	MNHN-IU-2011–3081	Papua New Guinea / 2010	KP759353	KP725471	KP725668	KP726043	N	N	Aznar-Cormano *et al*., 2015
Acanthephyra carinata	BSM110	Philippines	KP076184	KP075896	KP075798	KP076093	N	N	Wong *et al*., 2015
Acanthephyra cucullata	HBG925	Taiwan	KP076160	KP075893	KP075809	KP076110	N	N	Wong *et al*., 2015
Acanthephyra curtirostris	HBG1407	Gulf of Mexico	KP076161	KP075889	KP075807	KP076088	KP076029	N	Wong *et al*., 2015
Acanthephyra eximia	MNHN-IU-2008–16779/ NTOU M00709	Pacific Ocean: Southern Archipelago / 2002	KP759360	KP725477	KP725675	KP726049	EU427181	EU427250	Aznar-Cormano *et al*., 2015; Tsang *et al*., 2008
Acanthephyra fimbriata	HBG927	Philippines	KP076185	KP075895	KP075788	KP076092	N	N	Wong *et al*., 2015
Acanthephyra indica	MNHN-IU-2008–10188/ ACP16	Mozambique Channel / 2009	MW043001	MW043445	MW043460	MW052287	MW052301	MW052314	This study
Acanthephyra media	HBG930	Philippines	KP076166	KP075892	KP075805	KP076086	N	N	Wong *et al*., 2015

Table 2. Continued

| Species	Voucher No	Locality/year	GenBank accession numbers						References
			COI	16S	18S	H3	NaK	PEPCK	
Acanthephyra pelagica	HBG153	North Atlantic	KP076182	KP075880	KP075789	KP076100	KP076027	N	Wong et al., 2015
Acanthephyra purpurea	HBG899A	Gulf of Mexico	KP076170	KP075882	KP075782	KP076095	KP076023	N	Wong et al., 2015
Acanthephyra quadrispinosa	HBG931	Taiwan	KP076178	KP075886	KP075821	KP076099	KP076025	N	Wong et al., 2015
Outgroups									
Janicella spinicauda	HBG7002, HBG905 and MNHN-IU-2014–18783/ Op11	Gulf of Mexico, Papua New Guinea	MH572546	KP075932	MH100869	MH107256	N	N	Wong et al., 2015; Lunina et al., 2019b; Published in GenBank, Wilkins & Bracken-Grissom, 2020
Oplophorus gracilirostris	HBG909A and HBG904A	Gulf of Mexico	KP076150	KP075920	KP075847	KP076072	KP076045	N	Wong et al., 2015
Systellaspis pellucida	HBG944 and NTOU:M01001	Taiwan	KP076147	KP075924	JF346250	JF346319	JF346355	JF346391	Li et al., 2011; Wong et al., 2015

Sequences obtained in this work are indicated in bold. An 'N' designates gene sequences we were unable to acquire.

within the genus are robust: '*Acanthephyra armata*', '*Acanthephyra media*' and '*Acanthephyra purpurea*' species groups (Fig. 4). The ML tree shows lesser support (slightly below accepted 70) of the two deepest nodes indicated by arrows in Fig. 4. In other respects, ML and BI trees are similar.

MORPHOLOGICAL SYNAPOMORPHIES

MP trees are similar in Analyses 1–3 and we, therefore, mapped morphological synapomorphies in a single picture Fig. 5 for all analyses. In addition to robust clades shown in Fig. 3, all morphological analyses retrieved three minor clades within *Acanthephyra*, which do not receive statistical support but are identical to species groups retrieved in molecular analyses: '*Acanthephyra armat*', '*Acanthephyra media*' and '*Acanthephyra purpurea*' (Fig. 5). Unlike its position on the molecular trees, the first species group was combined with *Kemphyra*.

The clade 'Acanthephyridae without *Hymenodora*' is supported by the presence of the postorbital dorsal teeth on the rostrum (character 5, see Supporting Information, Appendix S1), a submarginal papilla and a lamina on the second maxilla (63), three-segmented endopod on the first maxilliped (65, 66) and a reduced dactyl of the fifth pereopods attached transversely to the propodus (91, 92). *Ephyrina* is supported by a rostrum shaped as an unarmed crest (0, 4), a postorbital ridge from the orbit to the posterior margin of the carapace and a blunt ridge ventral to the postorbital ridge (20, 23), a mandible unarmed along the distal margin (61), greatly compressed and expanded meri and ischia on all pereopods (75, 76, 81–86, 88, 89). The clade *Meningodora* + *Notostomus* is supported by a net of sharp lateral carinae along the whole carapace length (7, 8), including a sharp postorbital carina from the orbit to the posterior margin of the carapace (18) and a sharp oblique transverse carina ventral of the postorbital carina (24). In addition, *Meningodora* + *Notostomus* have a mandible unarmed along the distal margin (61), similar to that in *Ephyrina*. *Meningodora* is supported by a reduction of the dorsal carina on the second pleonic segment (35) and a blunt, indistinct carina on the third pleonic segment (38, 39). *Notostomus* is supported by a long branchiostegal carina, which is 0.7–1.0 of the carapace length (13), a supraorbital carina extending from the rostrum to the postorbital region (15), an additional lateral carina on posterior part of the carapace parallel to the postorbital carina (21) and a strong mesial teeth on the posterior margin of the third and fourth pleonic segments (44, 47). All these synapomorphies are stable within clades, except the presence of the postorbital dorsal teeth on the rostrum in the clade 'Acanthephyridae without *Hymenodora*': the teeth posteriorly disappear
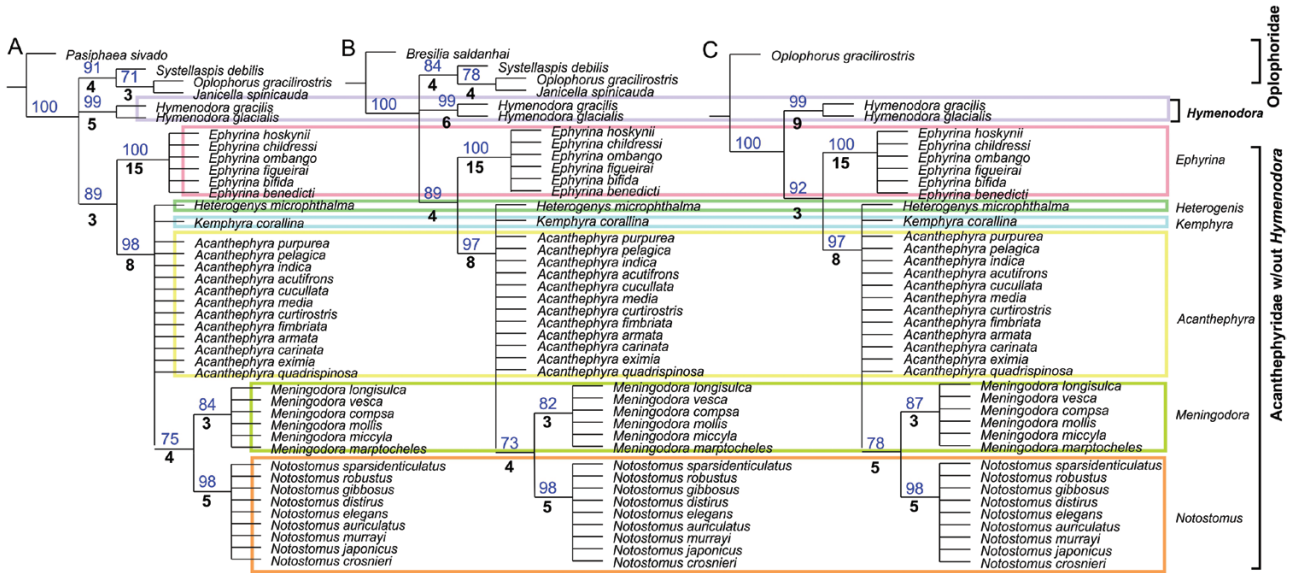
Figure 3. Morphological MP trees with *Janicella spinicauda* (A), *Oplophorus gracilirostris* (B) and *Systellaspis pellucida* (C) as the outgroups. Different colours indicate different genera. Only clades supported by both Bremer values (in bold, below branches) and bootstrap values (blue, above branches) are shown.

Table 3. Partitioning scheme and best models selected by PartitionFinder2

Partition	Best Model
16S	GTR+I+G
18S, 1st codon of *H3*	TRN+G
2nd codon of *H3*	K80+I
3rd codon of *H3*	GTR+G
1st codon of *COI*	SYM+I+G
2nd codon of *COI*	TVM+G
3rd codon of *COI*	GTR+G
1st codon of NaK, 1st codon of PEPCK	TVM+I+G
2nd codon of NaK	GTR+I
3rd codon of NaK	HKY+G
2nd codon of PEPCK	TVMEF+I
3rd codon of PEPCK	TVM+G

in *Ephyrina*. The mandible, unarmed along the distal margin, is a homoplasy found in the *Ephyrina* and *Meningodora* + *Notostomus* clades.

We grouped morphological synapomorphies into four types (Fig. 2) and calculated the contribution of each type in the support of major clades (Table 4 based on Fig. 5 and Supporting Information, Appendix 4). Average contribution of each type of synapomorphies ranged between 14% and 37% (last line in Table 4), but supporting synapomorphies were unevenly distributed in the analysed clades. The support of the *Ephyrina* clade was mainly provided by

synapomorphies linked to the pereopods (oar-like meri and ischia): their contribution was exceptionally high (67% vs. 14% on average). Meanwhile, the clades *Meningodora* + *Notostomus*, *Meningodora* and *Notostomus* were mainly supported by synapomorphies linked to strengthening of the carapace, pleon and telson (carinae and teeth), their combined contribution was greater than on average (80–100% vs. 32–37%).

DISCUSSION

EPHYRINA, *MENINGODORA* AND *NOTOSTOMUS* ON PHYLOGENETIC TREES AND THEIR STATUS

The most comprehensive analysis of Acanthephyridae hitherto done (Wong *et al.*, 2015) encompassed seven species of the target genera and 14 other species of the family: *Hymenodora* (two species), *Ephyrina* (three), *Meningodora* (two), *Notostomus* (two), *Heterogenys* (one) and *Acanthephyra* (11); the analysis was based on seven gene markers and did not include morphological evidence. Here we use six gene markers and significantly extended the number of analysed species of the target group (to 15) and the rest of Acanthephyridae (to 17, including a representative of the genus *Kemphyra* not sequenced before this study). In order to improve the power of the analyses, we also included morphological evidence.

Overall, our study makes the phylogenetic results shown in Fig. 2 by Wong *et al.* (2015) statistically significant. First, the major clades 'Acanthephyridae
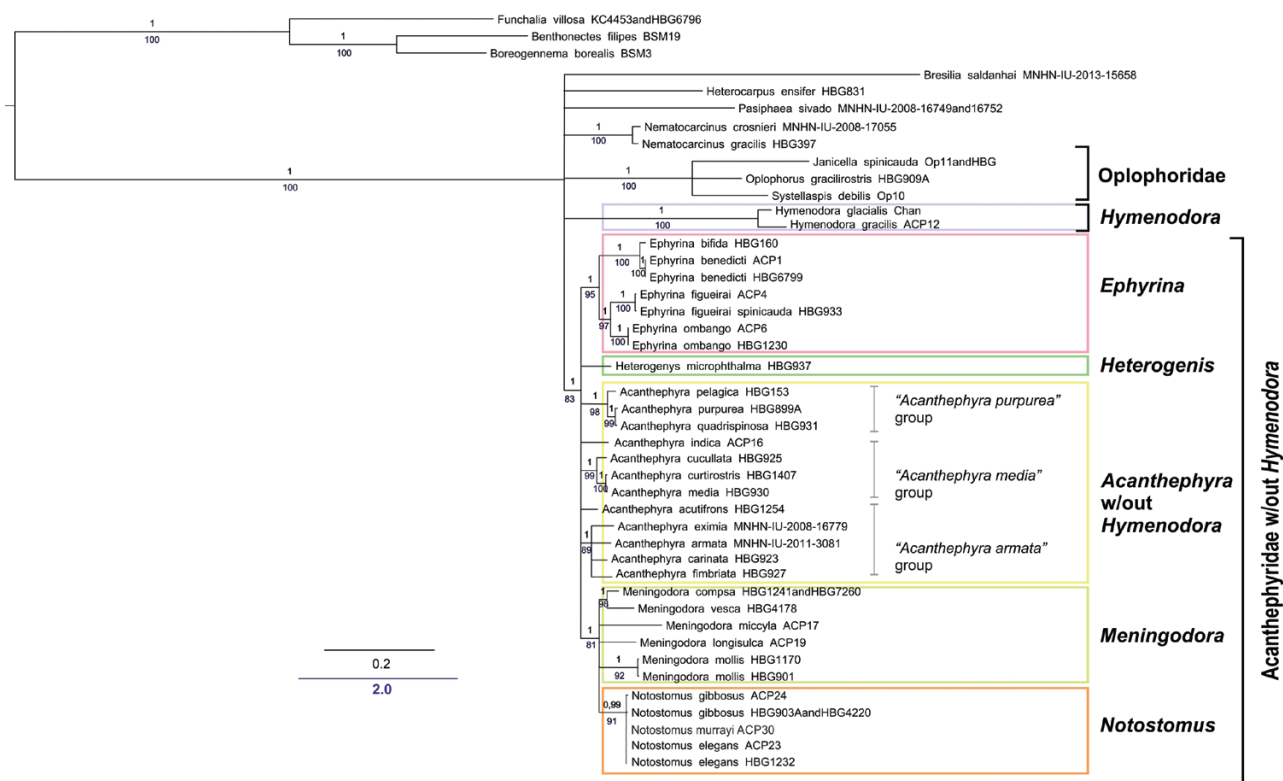
Figure 4. Molecular BI tree with supported clades, the horizontal scale bars mark the number of expected substitutions per site. Statistical support indicated as Bayesian posterior probabilities (black, above branches) and ML bootstrap analysis (blue, below branches). Different colours indicate different genera. Arrows indicate deep nodes perfectly resolved on the BI tree and insufficiently resolved on the ML tree.

without *Hymenodora*' and '*Heterogenys + Kemphyra + Acanthephyra + Notostomus + Meningodora*' are not robust on the BI tree in Wong *et al.* (2015) but gain support here. Both clades have great support on the BI molecular tree (0.98 and 1, Fig. 4) and high Bremer and bootstrap support on all morphological trees in Analyses 1–3 (Fig. 3). Having this in mind, we consider both deepest nodes on the tree (arrows in Fig. 4) resolved, although bootstrap values on the ML molecular tree are below the generally accepted 70 (68 and 63). Our results thus confirm that *Hymenodora* is a sister-clade to the rest of Acanthephyridae and that *Ephyrina* is a sister-clade to '*Heterogenys + Kemphyra + Acanthephyra + Notostomus + Meningodora*'.

As in Fig. 2 by Wong *et al.* (2015), the clade *Notostomus + Meningodora* is robust; this clade gains greater support on both of our molecular trees and is robust on all morphological trees. As in the previous studies, *Notostomus* is monophyletic in all trees and *Meningodora* is not resolved on both molecular trees. However, *Meningodora* is monophyletic and gains bootstrap and Bremer support on our morphological trees, which shows the resolving power of morphological methods in this particular case. The

current phylogenetic status of *Meningodora* match the status of *Systellaspis* (Lunina *et al.*, 2019b) from the sister-clade Oplophoridae: both genera are robust on the morphological trees and do not receive support on the molecular trees. As in Lunina *et al.* (2019b), we maintained a conservative approach and did not change the taxonomic status of *Meningodora*. We hope to solve the problem of a possible polyphyly of *Meningodora* and *Systellaspis* after completing a revision of the whole superfamily Oplophoroidea. *Ephyrina* and *Notostomus* are monophyletic genera on all trees.

Molecular methods, in turn, show the resolving power in a retrieving of statistical support for three species group clades within *Acanthephyra* (Fig. 4), which do occur (Fig. 5) but are not robust on the morphological trees (Fig. 3). Future use of the combination of morphological and molecular methods based on richer datasets and focused on *Acanthephyra* is needed to justify the taxonomic status of these species groups.

We conclude that the target group *Ephyrina–Notostomus–Meningodora* is not monophyletic on all phylogenetic trees and the unusual mandible and strengthened carapace observed in these genera thus
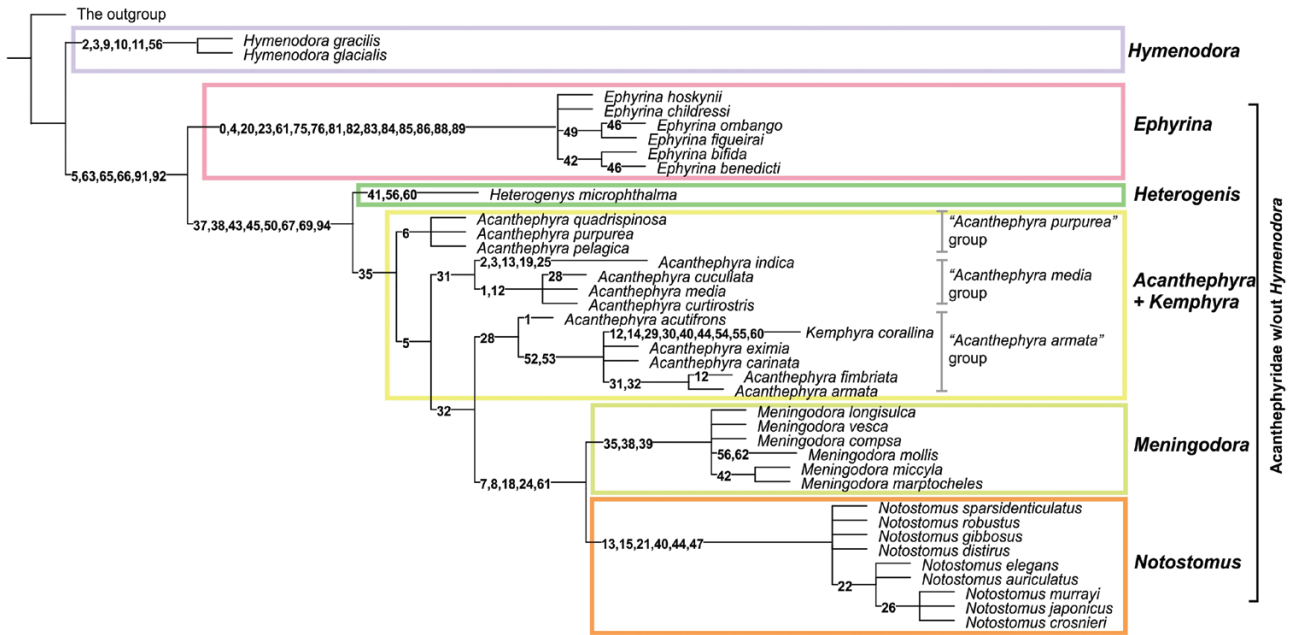
Figure 5. Synapomorphies on identical morphological MP trees with *Janicella spinicauda*, *Oplophorus gracilirostris* and *Systellaspis pellucida* as the outgroup. Different colours indicate different genera. Synapomorphies retrieved in analyses 1–3 are similar and mapped in Supporting Information, Appendix S4. Character coding see in Supporting Information, Appendix S1.

Table 4. Contribution (%) of different groups of synapomorphies supporting major clades of Acanthephyridae, results of morphological analyses 1–3 combined

Clades	Synapomorphies and their numerical order in parenthesis (see Appendix S1)			
	Carapace (0–32)	Pleon + telson (33–55)	Mouthparts (58–74)	Pereopods (75–92)
Hymenodora	83	0	17	0
Acanthephyridae without *Hymenodora*	17	0	50	33
Ephyrina	27	0	7	67
Acanthephyridae without *Hymenodora* and *Ephyrina*	0	71	29	0
Meningodora + Notostomus	80	0	20	0
Meningodora	0	100	0	0
Notostomus	50	50	0	0
Average for clades	**37**	**32**	**17**	**14**

exemplify parallel evolution. We reject the hypothesis of the monophyly of the target group.

MORPHOLOGICAL TRAITS IN *EPHYRINA*, *MENINGODORA* AND *NOTOSTOMUS*

Evolutionary traits in the clades *Ephyrina* and *Meningodora + Notostomus* are different. *Ephyrina* is mostly supported by synapomorphies linked to the pereopods: contribution of these characters is nearly five times higher than on average in the major clades of Oplophoroidea (Table 4). All meri and ischia in *Ephyrina* are greatly compressed, expanded and resemble oars (Fig. 1E) adapted to locomotory function. Unlike the usual spear-like and serrate shrimp rostra (Fig. 1C, 1D), the rostrum in *Ephyrina* is a smooth, wide lamina (Fig. 1E), possibly adapted to stabilize forward motion, as does a stempost of a cruiser. The forward motion requires strengthening of the carapace but not in the form of sharp carinae, which may cause

turbulent flow along carapace and pleon. *Ephyrina* has smooth ridges on the carapace extending from the orbit to the posterior margin, a blunt ridge ventral to the postorbital ridge (Fig. 1E) and no more ridges, carinae or teeth on the pleon. *Ephyrina benedicti* Smith, 1885 and *E. bifida* Stephensen, 1923 have 'dorsomedial teeth' on the third pleonic segment but these teeth are soft protuberances flattened dorsoventrally, adjacent to the pleon and do not prevent an active forward motion.

Our data suggest that the set of characters above evolved as a single morphological unit and contributed to the evolutionary success of the genus. Once evolved, this set of adaptations remained conservative and the six known species of *Ephyrina* are similar externally. Morphological traits within the genus mainly encompass development and the shape of dorsal protuberances on the third abdominal segment in two species (entire in *E. benedicti* and bifid in *E. bifida*) and spination of the telson: position of spines (dorsolateral in *E. bifida*, *E. childressi* Chace, 1986 and *E. hoskynii* Wood-Mason, 1891 or marginal in *E. benedicti*, *E. figueirai* Crosnier & Forest, 1973 and *E. ombango* Crosnier & Forest, 1973), number of spines and additional rows of spines (*E. figueirai*).

The *Meningodora* + *Notostomus* clade is mostly supported by synapomorphies linked to the strengthening of the carapace; contribution of these characters is two to three times higher than on average in the major clades of Oplophoroidea (Table 4). The strengthening is provided by means of sharp lateral carinae along the whole carapace length (a postorbital carina from the orbit to the posterior margin, an oblique transverse carina ventral of the postorbital carina; Fig. 1C, 1D), which are coupled with a thin, half-membranous integument. The strengthening has probably evolved to keep the body firm and rigid. Strong carinae on the carapace are likely analogous to stiffening members in ships and serve to reduce vibrations and flexing during fast movement (especially escape flips). Sharp carinae, which are absent in shrimps with a firm carapace, such as Oplophoridae and most Acanthephyridae, become indispensable for *Meningodora* and *Notostomus* having a thin and half-membranous integument.

The main evolutionary traits within the clade are linked to a further strengthening of the carapace and the pleon. *Notostomus* is supported by an impressive set of such synapomorphies (Fig. 1C) (the last two may also be defensive):

- A sharp branchiostegal carina along 0.7–1.0 of carapace length.
- An additional lateral carina on the posterior part, parallel to the postorbital carina.

- A supraorbital carina, extending from the rostrum to the postorbital region.
- A denticulate dorsal carina on the carapace.
- Strong and firm posteromesial teeth on the third to fifth abdominal somites.

The basic morphological trait within *Notostomus* is also linked to further strengthening of the carapace: *N. auriculatus* Barnard, 1950, *N. crosnieri* Macpherson, 1984, *N. elegans* A. Milne-Edwards, 1881, *N. japonicus* Spence Bate, 1888 and *N. murrayi* Spence Bate, 1888 have an additional lateral carina along the entire carapace length between the branchiostegal carina and the ventral margin of the carapace, the three latter species also have a transverse oblique carina extending dorsally from the postorbital carina (Fig. 1C). In other respects, all species of *Notostomus* are similar on the exterior and variations encompass proportions of carinae, denticulation of the carapace and the first abdominal somite.

Meningodora is supported by synapomorphies linked to a reduction of the dorsal pleonic carinae (absent on the second segment, blunt and indistinct on the third segment). The genus encompasses species smaller than *Notostomus*, which may partly explain the absence of the further strengthening observed in *Notostomus*. However, some strengthening is still observed in larger species: a long, sharp branchiostegal carina on the carapace (~half of the carapace length) in *M. mollis* Smith, 1882 and *M. compsa* (Chace, 1940) (Fig. 1D), and an armament of the third pleonic somite [posterodorsal tooth in *M. marptocheles* (Chace, 1940) and *M. miccyla* (Chace, 1940)]. There is an interesting trend linked to *M. mollis*, which occurs deeper than other *Meningodora* (Crosnier & Forest, 1973): this shrimp has a soft body and reduced cornea owing to the deep-living mode of this species. Another trait in *Meningodora* concerns relative length of the sixth and the fifth pleonic somites: the ratio is 1–1.5 in *M. compsa*, 1.5–2 in *M. longisulca* Kikuchi, 1985 and > 2 in the rest of the genus. We suggest that this row mirrors increasing movability of the species.

Overall, in the revised group, we observe different evolutionary traits. The first one is linked to an armament of the carapace and pleon with strong and numerous spines and ridges. This trait, likely associated with a defensive function and recorded here in *Notostomus*, was previously found in other pelagic crustaceans, such as Euphausiacea (Vereshchaka *et al.*, 2019a) and Oplophoridae (Lunina *et al.*, 2019b). The second trait is morphologically opposite to the first one and is linked to a 'smoothening' of the body (reduction of the spines and carinae). This trait, found here in *Ephyrina*, was previously recorded in the pelagic branch of Benthesicymidae

(Lunina *et al.*, 2019a; Vereshchaka *et al.*, 2020). Analyses of the '*Notostomus + Meningodora*' clade retrieved a novel evolutionary trait associated with keeping the body firm and rigid. The shrimps of this clade occur in the deep-sea and have a half-membranous carapace and pleon, which provide nearly zero buoyancy and, consequently, a reduction of energy loss. Strong carinae on their carapace and pleon may serve as a compensatory structure to provide a necessary supporting structure for locomotion.

A key to species of *Ephyrina*, *Meningodora* and *Notostomus* may be found in Chace (1986); the only species described since then is *M. longisulca*, which differs from all other *Meningodora* in the absence of the branchiostegal carina and in the unique (for *Meningodora*) ratio between the sixth and the fifth pleonic somites (1.7).

THE UNUSUAL MANDIBLE: AN EXAMPLE OF A PARALLEL EVOLUTION

In addition to the synapomorphies discussed above, the clades *Ephyrina* and *Meningodora + Notostomus* are supported by such a character as the unusual mandible (Fig. 1B), which is easily distinguishable from the mandibles of other decapods (Fig. 1A). We suggest that the characteristic mandibles have evolved in the *Ephyrina* and *Meningodora + Notostomus* clades independently as adaptations to feeding on an unusual prey. Indeed, most caridean pelagic shrimps (families Pasiphaeidae, Oplophoridae and Acanthephyridae) are voracious predators, living on small fish, decapods and euphausiids (e.g. review in: Burukovsky, 2009). In particular, Burukovsky (2009) studied in detail the gut content of such representatives of Oplophoroidea as *Systellaspis* [*S. debilis* (A. Milne-Edwards, 1881), *S. pellucida*], *Acanthephyra* [*A. acanthitelsonis* Spence Bate, 1888, *A. eximia* Smith, 1884, *A. fimbriata* Alcock & Anderson, 1894, *A. kingsleyi* Spence Bate, 1888, *A. pelagica* (Risso, 1816) and *A. purpurea* A. Milne-Edwards, 1881] and *Oplophorus* [*O. gracilirostris*, *O. novaezealandiae* (de Man, 1931), *O. spinosus* (Brullé, 1839) and *O. typus* H. Milne-Edwards, 1837], and found that the most common and voluminous dietary items of all these decapods are fish and crustaceans. Shrimps have typical oplophoroid mandibles (reduced molar process and subtriangular incisor process armed with teeth along the entire inner margin; Fig. 1A), which can crush crustacean carapaces and fish bones and further cut tissues.

The prey of *Ephyrina*, *Meningodora* and *Notostomus* is different. Although the feeding of these genera is underexplored, scattered information confirms our suggestion about their different trophic specializations. Examination of the gut content of *Notostomus* (*N. crosnieri* and *N. elegans*), *Ephyrina figueirai* and *Meningodora vesca* shows that the most common and voluminous dietary items of these species differ from those found in other pelagic decapods and are represented by pelagic cnidarians (Burukovsky, 2009). Other studies also indicate that cnidarian tissue is the most common dietary item of *Notostomus japonicus* (Nishida *et al.*, 1988). *Notostomus robustus* Smith, 1884 has even been observed from a submersible feeding on the medusa *Atolla wyvillei* Haeckel, 1880 (Moore *et al.*, 1993). Our study is first to emphasize a link between this type of mandible (Fig. 1B) and feeding on gelatinous organisms but no direct observations on feeding procedure of deep-sea *Notostomus*, *Meningodora* or *Ephyrina* have been made (if possible at all). We may only hypothesize that a sharp, smooth blade is more efficient for the destruction of voluminous soft tissues (feeding objects are large enough) than a thickened serrate margin (teeth are buttressed by a relief). A sharp, smooth blade likely chops tissues (as we use a smooth acute knife to cut butter), whereas a serrated blade saws and crushes tissues (like when we slice bread).

Overall, during colonization of the pelagic realm, the main trophic trend in the evolution of pelagic decapods, including Oplophoroidea, was linked to feeding on crustaceans and fish that was mirrored in the mandible with subtriangular and an entirely serrated incisor process. Two clades of Oplophoroidea, *Ephyrina* and *Meningodora + Notostomus*, followed another trophic pathway. They feed, presumably, on gelatinous animals, mainly cnidarians, thus filling a separate ecological niche. Gelatinous animals, which significantly contribute to the pelagic biomass in all depth zones (Vereshchaka *et al.*, 2016), are consumed by a limited number of predators and thus represent a potentially strong food source. Noteworthy, *Notostomus* is dominant in the meso- and upper bathypelagic of the Subequatorial and Equatorial Atlantic in terms of biomass (Vereshchaka *et al.*, 2019b). The unusual mandibles that evolved in the clades *Ephyrina* and *Meningodora + Notostomus*, therefore, represent a remarkable example of parallel evolution.

CONCLUSIONS

Here we present the first comprehensive phylogenetic revision of the genera *Ephyrina*, *Meningodora* and *Notostomus* based on the synchronous use of 95 morphological characters (all valid species included) and six gene markers (71% of valid species belonging to the target genera included). These three genera have an unusual carapace strengthened with a set of ridges and carinae, and a one-sided serrated mandible, which suggest possible monophyly of this group; a hypothesis we test here.

It is noteworthy that both morphological and molecular analyses retrieve trees with similar topology and a set of statistically supported clades. We show that *Ephyrina* and *Meningodora* + *Notostomus* are separate clades and thus reject the hypothesis of group monophyly. The genera *Ephyrina* and *Notostomus* are monophyletic, both on the morphological and on molecular trees; *Meningodora* gains support only on the morphological trees.

Basic evolutionary traits in the *Ephyrina* and *Meningodora* + *Notostomus* clades are different. In *Ephyrina*, they are mostly linked to the pereopods (oar-like) and shape of the rostrum (smooth lamina possibly acting as a stempost) favouring active forward motion. The *Meningodora* + *Notostomus* clade is predominantly supported by synapomorphies coupled with the carapace and pleon strengthened with ridges and carinae, which is indispensable for *Meningodora* and *Notostomus* with their half-membranous integument. Carapace strengthening further evolved into an even more elaborate net of sharp carinae in large *Notostomus* as a possible response to increasing carapace loads.

Our results suggest that unusual mandibles evolved in the clades *Ephyrina* and *Meningodora* + *Notostomus* independently and represent convergent trophic adaptations. Unlike most pelagic decapods feeding on other crustaceans and fish, both clades follow an alternative pathway and are adapted to feeding on gelatinous organisms, mostly cnidarians. Living on this prey appears to be ecologically advantageous, as species of *Notostomus* dominate in the low-latitude Atlantic communities in terms of biomass.

ACKNOWLEDGEMENTS

DATA ACCESSIBILITY

Our data will be deposited in the Dryad Digital Repository.

REFERENCES

Apakupakul K, **Siddall ME**, **Burreson EM. 1999.** Higher level relationships of leeches (Annelida: Clitellata: Euhirudinea) based on morphology and gene sequences. *Molecular Phylogenetics and Evolution* **12:** 350–359.

Aznar-Cormano L, **Brisset J**, **Chan TY**, **Corbari L**, **Puillandre N**, **Utge J**, **Zbinden M**, **Zuccon D**, **Samadi S. 2015.** An improved taxonomic sampling is a necessary but not sufficient condition for resolving inter-families relationships in Caridean decapods. *Genetica* **143:** 195–205.

Bracken HD, **De Grave S**, **Felder DL. 2009.** Phylogeny of the infraorder Caridea based on nuclear and mitochondrial genes (Crustacea: Decapoda). In: Martin JW, Crandall KA, Felder DL, eds. *Decapod crustacean phylogenetics (Crustacean issue 18)*. Boca Raton: CRC Press, 274–300.

Bracken-Grissom HD, **Felder DL**, **Vollmer NL**, **Martin JW**, **Crandall KA. 2012.** Phylogenetics links monster larva to deep-sea shrimp. *Ecology and Evolution* **2:** 2367–2373.

Bracken-Grissom HD, **Ahyong ST**, **Wilkinson RD**, **Feldmann RM**, **Schweitzer CE**, **Breinholt JW**, **Bendall M**, **Palero F**, **Chan TY**, **Felder DL**, **Robles R**, **Chu KH**, **Tsang LM**, **Kim D**, **Martin JW**, **Crandall KA. 2014.** The emergence of lobsters: phylogenetic relationships, morphological evolution and divergence time comparisons of an ancient group (decapoda: achelata, astacidea, glypheidea, polychelida). *Systematic Biology* **63:** 457–479.

Burukovsky RN. 2009. *Feeding and trophic relations of shrimps*. Izdatelstvo FGOU VPO' KGTU'. [in Russian].

Chace FA.1986. *The caridean shrimps (Crustacea: Decapoda) of the Albatross Philippine Expedition, 1907–1910, Part 4: families oplophoridae and nematocarcinidae*. Washington, DC: Smithsonian Institution Press.

Chan TY, **Lei HC**, **Li CP**, **Chu KH. 2010.** Phylogenetic analysis using rDNA reveals polyphyly of Oplophoridae (Decapoda: Caridea). *Invertebrate Systematics* **24:** 172–181.

Colgan DJ, **McLauchlan A**, **Wilson GDF**, **Livingston SP**, **Edgecombe GD**, **Macaranas J**, **Gray MR. 1998.** Histone H3 and U2 snRNA DNA sequences and arthropod molecular evolution. *Australian Journal of Zoology* **46:** 419–437.

De Grave S, **Pentcheff D**, **Ahyong ST. 2009.** A classification of living and fossil genera of decapod crustaceans. *Raffles Bulletin of Zoology* **21 (Supplement):**1–109.

Ditter RE, **Mejía-Ortíz LM**, **Bracken-Grissom HD. 2020.** Anchialine adjustments: an updated phylogeny and classification for the family Barbouriidae Christoffersen, 1987 (Decapoda: Caridea). *Journal of Crustacean Biology* **40:** 401–411.

Edgar RC. 2004. MUSCLE: multiple sequence alignment with high accuracy and high throughput. *Nucleic Acids Research* **32:** 1792–1797.

Edler D, **Klein J**, **Antonelli A**, **Silvestro D. 2020.** RaxmlGUI 2.0 beta: a graphical interface and toolkit for phylogenetic analyses using RAxML. *Methods in Ecology and Evolution.* Doi:10.1111/2041-210X.13512.

Felder DL, **Robles R. 2009.** Molecular phylogeny of the family Callianassidae based on preliminary analyses of two mitochondrial genes. In: Martin JW, Crandall KA, Felder DL, (eds). *Decapod crustacean phylogenetics (Crustacean issue 18).* Boca Raton: CRC Press, 319–334.

Folmer O, **Black M**, **Hoeh W**, **Lutz R**, **Vrijenhoek R. 1994.** DNA primers for amplification of mitochondrial cytochrome c oxidase subunit I from diverse metazoan invertebrates. *Molecular Marine Biology and Biotechnology* **3:** 294–299.

Goloboff P, **Farris S**, **Nixon K. 2000.** *TNT: tree analysis using new technology.* Available at: http://www.lillo.org.ar/phylogeny/tnt/.

Kumar S, **Stecher G**, **Li M**, **Knyaz C**, **Tamura K. 2018.** MEGA X: Molecular evolutionary genetics analysis across computing platforms. *Molecular Biology and Evolution* **35:** 1547–1549.

Lanfear R, **Frandsen PB**, **Wright AM**, **Senfeld T**, **Calcott B. 2016.** PartitionFinder 2: new methods for selecting partitioned models of evolution for molecular and morphological phylogenetic analyses. *Molecular Biology and Evolution* **34:** 772–773.

Li CP, **De Grave S**, **Chan TY**, **Lei HC**, **Chu KH. 2011.** Molecular systematics of caridean shrimps based on five nuclear genes: implications for superfamily classification. *Zoologischer Anzeiger-A Journal of Comparative Zoology* **250:** 270–279.

Lunina AA, **Kulagin DN**, **Vereshchaka AL. 2019a.** A hard-earned draw: phylogeny-based revision of the deep-sea shrimp *Bentheogennema* (Decapoda: Benthesicymidae) transfers two species to other genera and reveals two new species. *Zoological Journal of the Linnean Society* **187:** 1155–1172.

Lunina AA, **Kulagin DN**, **Vereshchaka L. 2019b.** Oplophoridae (Decapoda: Crustacea): phylogeny, taxonomy and evolution studied by a combination of morphological and molecular methods. *Zoological Journal of the Linnean Society* **186:** 213–232.

Moore PG, **Rainbow PS**, **Larson RJ. 1993.** The mesopelagic shrimp *Notostomus robustus* Smith (Decpoda: Oplophoridae) observed in situ feeding on the medusa *Atolla wyfilei* Haeckel in the northwest Atlantic, with notes on gut contents and mouthpart morphology. *Journal of Crustacean Biology* **13:** 690–696.

Nishida S, **Pearcy WG**, **Nemoto T. 1988.** Feeding habits of mesopelagic shrimps collected off Oregon. *Bulletin of the Ocean Research Institute, University of Tokyo* **26:** 99–108.

Nixon K. 1999. The parsimony ratchet, a new method for rapid parsimony analysis. *Cladistics* **15:** 407–414.

Reuschel S, **Schubart CD. 2006.** Phylogeny and geographic differentiation of Atlanto-Mediterranean species of the genus *Xantho* (Crustacea: Brachyura: Xanthidae) based on genetic and morphometric analyses. *Marine Biology* **148:** 853–866.

Robles R, **Tudge CC**, **Dworschak PC**, **Poore GCB**, **Felder DL. 2009.** Molecular phylogeny of the Thalassinidea based on nuclear and mitochondrial genes. In: Martin JW, Crandall KA, Felder DL, eds. *Decapod crustacean phylogenetics (Crustacean issues 18).* Boca Raton: CRC Press, 301–318.

Ronquist F, **Teslenko M**, **van der Mark P**, **Ayres DL**, **Darling A**, **Höhna S**, **Larget B**, **Liu L**, **Suchard MA**, **Huelsenbeck JP. 2012.** MrBayes 3.2: efficient Bayesian phylogenetic inference and model choice across a large model space. *Systematic Biology* **61:** 539–542.

Schubart CD. 2009. Mitochondrial DNA and decapod phylogenies: the importance of pseudogenes and primer optimization. *Decapod Crustacean Phylogenetics* **47:** 65.

Schubart CD, **Huber MGJ. 2006.** Genetic comparisons of German populations of the stone crayfish, *Austropotamobius torrentium* (Crustacea: Astacidae). *Bulletin Français de la Pêche et de la Pisciculture* **380–381:** 1019–1028.

Schubart CD, **Cuesta JA**, **Felder DL. 2002.** Glyptograpsidae, a new brachyuran family from Central America: larval and adult morphology, and a molecular phylogeny of the Grapsoidea. *Journal of Crustacean Biology* **22:** 28–44.

Stamatakis A. 2014. RAxML version 8: a tool for phylogenetic analysis and post-analysis of large phylogenies. *Bioinformatics* **30:** 1312–1313.

Tsang LM, **Ma KY**, **Ahyong ST**, **Chan TY**, **Chu KH. 2008.** Phylogeny of Decapoda using two nuclear protein-coding genes: origin and evolution of the Reptantia. *Molecular Phylogenetics and Evolution* **48:** 359–368.

Toon A, **Finley M**, **Staples J**, **Crandall KA. 2009.** Decapod phylogenetics and molecular evolution. In: Martin JW, Crandall KA, Felder DL, eds. *Decapod crustacean phylogenetics (Crustacean issues 18).* Boca Raton: CRC Press, 14–28.

Vereshchaka AL, **Abyzova G**, **Lunina A**, **Musaeva E**, **Sutton T. 2016.** A novel approach reveals high zooplankton standing stock deep in the sea. *Biogeosciences* **13:** 6261–6271.

Vereshchaka AL, **Kulagin DN**, **Lunina AA**, **2019a.** A phylogenetic study of krill (Crustacea: Euphausiacea) reveals new taxa and co-evolution of morphological characters. *Cladistics* **35:** 150–172.

Vereshchaka AL, **Lunina A**, **Sutton T. 2019b.** Assessing deep-pelagic shrimp biomass to 3000 m in the Atlantic Ocean and ramifications of upscaled global biomass. *Scientific Reports* **9:** 5946.

Vereshchaka AL, **Corbari L**, **Kulagin DN**, **Lunina AA**, **Olesen J**, **2020.** A phylogeny-based revision of the shrimp genera *Altelatipes*, *Benthonectes* and *Benthesicymus* (Crustacea: Decapoda: Benthesicymidae). *Zoological Journal of the Linnean Society* **189:** 207–227.

Wong JM, **Pérez-Moreno JL**, **Chan TY**, **Frank TM**, **Bracken-Grissom HD. 2015.** Phylogenetic and transcriptomic analyses reveal the evolution of bioluminescence and light detection in marine deep-sea shrimps of the family Oplophoridae (Crustacea: Decapoda). *Molecular Phylogenetics and Evolution* **83:** 278–292.

WoRMS Editorial Board. 2020. *World register of marine species.* Available at: http://www.marinespecies.org at VLIZ (accessed 29 May 2020).

SUPPORTING INFORMATION

Additional Supporting Information may be found in the online version of this article at the publisher's web-site.

Appendix S1. Character scoring.
Appendix S2. Data matrix.
Appendix S3. Retrieved trees.
Appendix S4. Synapomorphies.